NASA TN D-453

TECHNICAL NOTE
D-453

LANDING ENERGY DISSIPATION FOR MANNED REENTRY VEHICLES

By Lloyd J. Fisher, Jr.

Langley Research Center
Langley Field, Va.

NATIONAL AERONAUTICS AND SPACE ADMINISTRATION
WASHINGTON September 1960

1J

NATIONAL AERONAUTICS AND SPACE ADMINISTRATION

TECHNICAL NOTE D-453

LANDING ENERGY DISSIPATION FOR MANNED REENTRY VEHICLES

By Lloyd J. Fisher, Jr.

SUMMARY

L1082

Analytical and experimental investigations have been made to determine the landing-energy-dissipation characteristics for several types of landing gear for manned reentry vehicles. The landing vehicles are considered in two categories: those having essentially vertical-descent paths, the parachute-supported vehicles, and those having essentially horizontal paths, the lifting vehicles. The energy-dissipation devices discussed are crushable materials such as foamed plastics and honeycomb for internal application in couch-support systems, yielding metal elements as part of the structure of capsules or as alternates for oleos in landing-gear struts, inflatable bags, braking rockets, and shaped surfaces for water impact.

It appears feasible to readily evaluate landing-gear systems for internal or external application in hard-surface or water landings by using computational procedures and free-body landing techniques with dynamic models. The systems investigated have shown very interesting energy-dissipation characteristics over a considerable range of landing parameters. Acceptable gear can be developed along lines similar to those presented if stroke requirements and human-tolerance limits are considered.

INTRODUCTION

The landing vehicles for manned reentry are considered in two categories: those having essentially vertical-descent paths, the parachute-supported vehicles, and those having essentially horizontal paths, the lifting vehicles. Because of the nature of the operation, numerous maintenance free landings are not required; consequently, one-shot landing gears having replaceable elements are particularly interesting. This paper presents some brief results from analytical and experimental investigations of energy dissipation with such landing gear in order to give a general idea of feasibility.

STATEMENT OF PROBLEM

The major variables of landing energy dissipation are velocity and stopping distance and the quantities to be determined as far as man is concerned are maximum acceleration, duration, and onset rate of acceleration. (See ref. 1.) Possible acceleration time histories for reentry landings are shown in figure 1. For orientation purposes typical accelerations are shown by the broken lines. Maximum acceleration and duration are apparent on a time history but onset rate is not so obvious. For purposes of this paper onset rate is considered as the ratio of plateau acceleration to time for reaching plateau. The plateau value is obtained by approximating the more complicated time histories with a simple trapezoid as shown by the solid line.

Acceleration and onset rate determine man's tolerance to impact and the physical relationship of these parameters shows what compromises can be made between the two for the stopping distances available. These relationships are shown in figure 2 where maximum acceleration in g units is plotted against stopping distance in inches. (See ref. 2.) The data shown are at an impact velocity of 30 ft/sec, a value familiar for parachute-supported vehicles. The lower curve is for an infinite onset rate and the curves for onset rates of 9,000, 1,500, and 400 g/sec are from trapezoidal acceleration time histories. The dashed curve represents a linear buildup to maximum acceleration at maximum time and with the curve for infinite onset rate forms a limit for the given conditions. A frequently quoted tolerance for man with load applied sternumward is shown by the point at 40g, 1,500 g/sec, and about $8\frac{1}{2}$ inches stopping distance. It should be realized that the stopping distances shown in this figure are the absolute minimum for the given conditions.

DISCUSSION

A short motion-picture film supplement illustrating the effects discussed in this paper has been prepared and is available on loan. A request card form and a description of the film will be found at the end of this paper, on the page immediately preceding the abstract and index pages.

Various energy-dissipation devices are being considered for manned reentry vehicles. Those receiving most attention presently are yielding metal elements as part of the structure of capsules or as alternates for oleos in landing gear struts, inflatable bags, crushable materials such as foamed plastics and honeycombs, braking rockets, and shaped surfaces for water impact.

L-1082

Couch Support

The crushable materials are receiving most attention for internal application in couch-support systems. It is difficult to scale such materials; therefore, full-scale testing appears best. Results from drop tests using a combination of semirigid plastic and aluminum honeycomb are given in figure 3. (See ref. 2.) The drop-test model consisted of 4 inches of each material with a metal plate separating the two. The static loading for the test weight was 1 psi. Aluminum honeycomb is an efficient material for impact load alleviation since up to 80 percent of its depth is usable and there is little rebound. However, the stiffness of the material results in high onset rates of acceleration. These may be controlled by reducing the initial area of contact, by precrushing, or by combining with foamed plastic as shown here. Plateau acceleration was about 30g and the onset rate was about 2,500 g/sec for this combination. The initial shape of the acceleration followed the simple one-degree-of-freedom spring constant for springs in series. One of the problems inherent in work of this nature is shown by the sharp peaks in the record indicating that the test weight "virtually" bottomed before the impact velocity had been completely dissipated.

Vertical-Landing Vehicles

It usually is feasible to absorb only part of the landing energy with coach or seat supports; therefore, some external absorption must be provided. The inflatable bag lends itself very well to energy absorption for the vertical-landing vehicle. Included in this category are the emergency escape pods and the reentry ballistic capsules. A number of bag shapes such as a cylinder, sphere, or torus might be used depending on design requirements. (See ref. 3.)

Torus-shaped bag.- A drawing of a model of a torus-shaped landing bag is shown in figure 4. This bag is divided into eight compartments, the partitions of which are shown by dashed lines in the plan view of the torus. The compartments are needed in cocked landings to permit pressure buildup under that part of the capsule impacting first. Each compartment has a blowout patch so that air can escape from the bag to regulate acceleration and prevent rebound. The patches are designed to blow out at scale pressure.

Sequence photographs of landings of the torus-bag model are given in figure 5. Figure 5(a) shows the model in a vertical flight path. The blowout patches (little white disks) can be seen just after blowout in the fourth picture of the sequence. Figure 5(b) shows the model in a 63° flight path. An additional air bag has been used in this condition to ease turnover impact. Turnover results if horizontal velocity is too great but turnover is a secondary problem which can be solved by the same technique used for the main air bag.

Figure 6 gives full-scale accelerations for torus bag landings at several attitudes in a flight path that would result from a horizontal wind velocity of about 9 knots. The positive and negative attitudes and axes of the capsule are illustrated by the sketches with direction of flight path shown by the arrows. These data are for a vertical impact velocity of 30 ft/sec, a flight-path angle of 60°, a vehicle weight of 1,200 pounds, and a 3.5-foot torus section diameter. The acceleration along the X-axis shows a maximum of about 30g (full scale) at a 0° landing with a decrease in acceleration as attitude is changed. The acceleration along the Z-axis is zero at a 0° landing and increases in magnitude as attitude is changed. Maximum onset rate for this air bag was about 600 g/sec.

L-1082

<u>Vertical-cylinder bag</u>.- A drawing of a vertical-cylinder landing-bag model is shown in figure 7. The air chamber upper body of the model is used to improve scaling accuracy and is not a part of an actual vehicle. The air bag is installed between the air chamber and a heat shield and is opened from a collapsed position by the weight of the heat shield. There is essentially unrestricted flow between the air bag and air chamber. Orifices which are always open are located around the upper part of the bag. The bag is dimensionally representative of a prototype 6 feet in diameter, 4 feet long, used with a 2,000-pound capsule.

An acceleration time history for this configuration in a landing on concrete at a flight-path angle of 90° (vertical) and a 0° contact attitude is given in figure 8. Computed and experimental results are in good agreement at model scale and scale up to full size as shown here. Comparisons with large-scale model tests also indicate agreement. This bag was designed for low accelerations and results in a maximum value of about 10g. Onset rate was about 200 g/sec. Landings at other flight-path angles and attitudes have shown similarly acceptable acceleration.

Computations of acceleration for the various systems discussed herein have been made at the 0° attitude, vertical flight-path condition only.

<u>Compliable metal legs</u>.- A drawing of a model used to investigate energy dissipation and scaling methods for compliable-metal-leg shock absorbers is shown in figure 9. The model consisted of a steel weight attached to a wooden base by 3003-H14 aluminum-alloy legs and weighed about 30 pounds. The legs were made of rectangular strips bent as shown. This initial bend was used in an attempt to reduce onset rate

and to control the location of bending during impact. A large-scale model similar to this one and weighing about 200 pounds was also tested.

Figure 10 gives an acceleration time history for the compliable-metal-leg models in landings on concrete. The small-scale-model data are shown by the long-dash—short-dash line and the large-scale-model data by the dashed line. The agreement is very good. The computed acceleration time history shown by the solid line uses a value of yield stress about one-fourth greater than the handbook value because of work hardening during fabrication, high strain rates during impact, and plastic flow.

L-1082

The onset rate of acceleration for these configurations is high, about 10,000 g/sec. Other investigations using tapered legs have given onset rates of about 2,000 g/sec for the same design maximum acceleration. A photograph showing the tapered compliable metal legs installed between a capsule and heat shield is shown as figure 11. The tapered legs are prebent into a modified "S" curve. Typical sequence photographs of a landing on concrete are given in figure 12.

<u>Water impact</u>.- Another method for landing a space capsule is the water landing. (The configurations discussed previously have lower accelerations in water landings than in hard-surface landings.) The water landing provides a way of obtaining long stroke without onboard devices, that is, by shaping the vehicle for water penetration. It is also of interest where accuracy for hitting a landing area is a question. Peak impact accelerations for two capsules landing on water are given in figure 13. (See refs. 4 and 5.) One capsule impacts on a 126-inch spherical radius heat shield and the other on a 53° conical heat shield. Both model and full-scale experimental investigations were made for the 126-inch spherical radius model. The model results are shown by the solid line and full-scale results by the dashed line. Experimental model results for the 53° conical model are shown by the lower solid line. Computed results for both configurations, by using well established procedures, are shown by the circles. Excellent agreement is indicated between model, full scale, and computation. The curves show that configuration shape has a significant influence on landing acceleration. At 0° contact attitude the 126-inch spherical radius model has a blunt shape, water penetration is small, and the peak acceleration is high. Onset rate is about 20,000 g/sec. As contact attitude changes from 0°, the accelerations decrease rapidly and onset rate also decreases to about 800 g/sec at a 30° contact attitude. The difference is due to the more pointed shape of the impacting surface as attitude increases. The 53° conical model has fairly low accelerations, about 10g, and shows little change with change in attitude. Onset rate is about 400 g/sec. The accelerations in the 10g region for both models result from fairly deep water penetration or in other words relatively long strokes.

Braking rocket.- Another long-stroke system for energy dissipation in a capsule landing is the braking rocket. This system employs rocket thrust alined with the flight path for stopping. If g tolerance for man is greatly reduced by long exposure to zero or very low gravity in space environment, the low landing accelerations possible with the braking rocket could be the answer for returning from such missions. Typical sequence photographs of a landing of a dynamic model using this system are given in figure 14. Only a very few landings have been made with this model but the behavior and control have been very good. A maximum acceleration of about 3g occurred in these tests. A change in landing condition such as an increase in speed would result in higher accelerations or would require more thrust or thrust duration than used in the test. Depending on design requirements, a wide range of acceleration and stroke is possible with the braking rocket. L-1082

Horizontal-Landing Vehicle

Each of the systems discussed has special advantages, as an example the compliable metal elements can be more adaptable to space environments than certain other systems, especially as alternates to oleos in shock-absorber struts. An application of the compliable metal principle similar to that already shown for a capsule has been investigated on a dynamic model of a horizontal-landing reentry vehicle. Figure 15 is a photograph of the model. The landing gear consists of a pair of main skids aft and a dual nose wheel with tires forward. Simple yielding metal strips are incorporated into the gear struts and they deform in bending during landing impact. Brief tests were also made with the nose wheel moved aft and with a nose skid replacing the original wheel.

Typical sequence photographs of a landing made with the main-skid nose-wheel landing gear are given in figure 16. The main gear contacts first, then the model trims down, and the nose wheel impacts; thus the shock strut is deformed.

A schematic time history of part of a landing is given in figure 17. Shown in this figure is attitude, accelerations at the nose gear, and accelerations at the main gear. At point 1, the main gear contacts the runway and the model trims down to nose-wheel impact at point 2. The nose-gear shock strut deformed during impact at point 2. At about the same time a reaction acceleration occurred which caused the main-gear struts to yield at point 3. During the nose-wheel impact the force or accelerations built up along an elastic line and upon reaching the yield stress of the strut remained fairly constant through the yield or deformation stroke. In the case of the main gear, the struts yield in the plastic range at a small value of acceleration, but the acceleration builds up again because the gear bottomed. Maximum landing acceleration always occurred at nose-gear impact and was about 5g. Moving the nose wheel aft or replacing the wheel with the nose skid had little effect on acceleration or stability.

CONCLUDING REMARKS

It appears feasible to readily evaluate landing-gear systems for internal or external application in hard-surface or water landings by computation methods and free-body landing techniques with dynamic models. The systems investigated have shown very interesting landing-energy-dissipation characteristics over a considerable range of landing parameters. Acceptable gear could be developed along lines similar to those presented if stroke requirements and human-tolerance limits are considered.

Langley Research Center,
National Aeronautics and Space Administration,
Langley Field, Va., April 12, 1960.

REFERENCES

1. Eiband, A. Martin: Human Tolerance to Rapidly Applied Accelerations: A Summary of the Literature. NASA MEMO 5-19-59E, 1959.

2. O'Bryan, Thomas C., and Hatch, Howard G., Jr.: Limited Investigation of Crushable Structures for Acceleration Protection of Occupants of Vehicles at Low Impact Speeds. NASA TN D-158, 1959.

3. Esgar, Jack B., and Morgan, William C.: Analytical Study of Soft Landings on Gas-Filled Bags. NASA TR R-75, 1960.

4. Vaughan, Victor L., Jr.: Water-Landing Impact Accelerations for Three Models of Reentry Capsules. NASA TN D-145, 1959.

5. McGehee, John R., Hathaway, Melvin E., and Vaughan, Victor L., Jr.: Water-Landing Characteristics of a Reentry Capsule. NASA MEMO 5-23-59L, 1959.

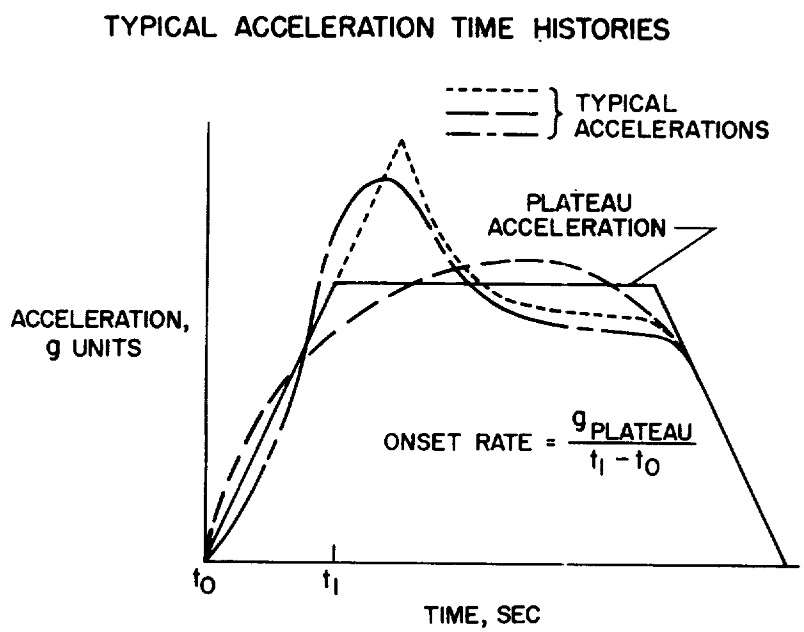

Figure 1

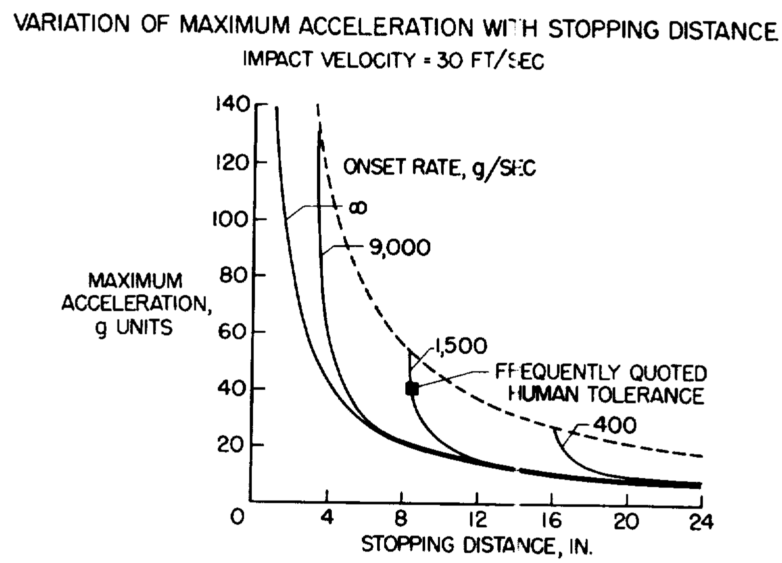

Figure 2

L-1082

L-1082

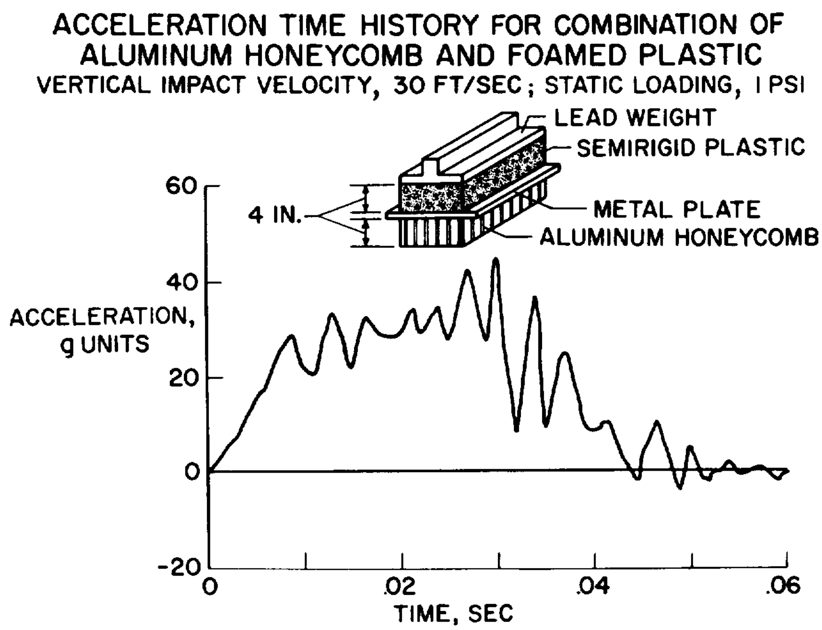

Figure 3

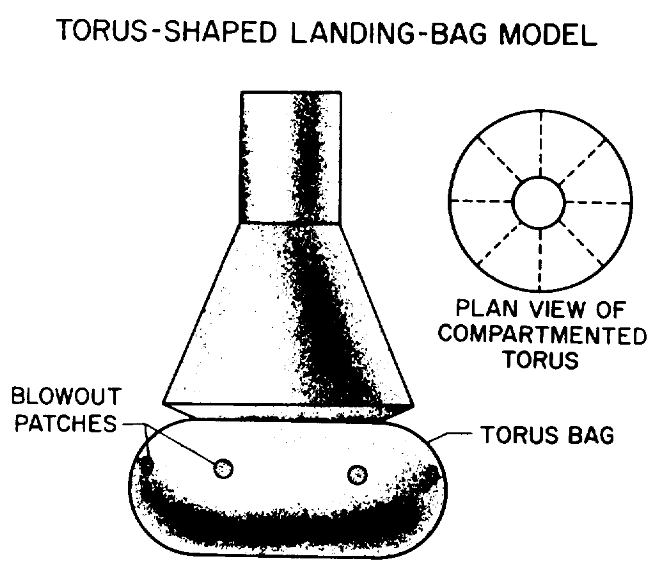

Figure 4

SEQUENCE OF TORUS BAG LANDINGS ON CONCRETE
FLIGHT-PATH ANGLE, 90° ; CONTACT ATTITUDE, 0°

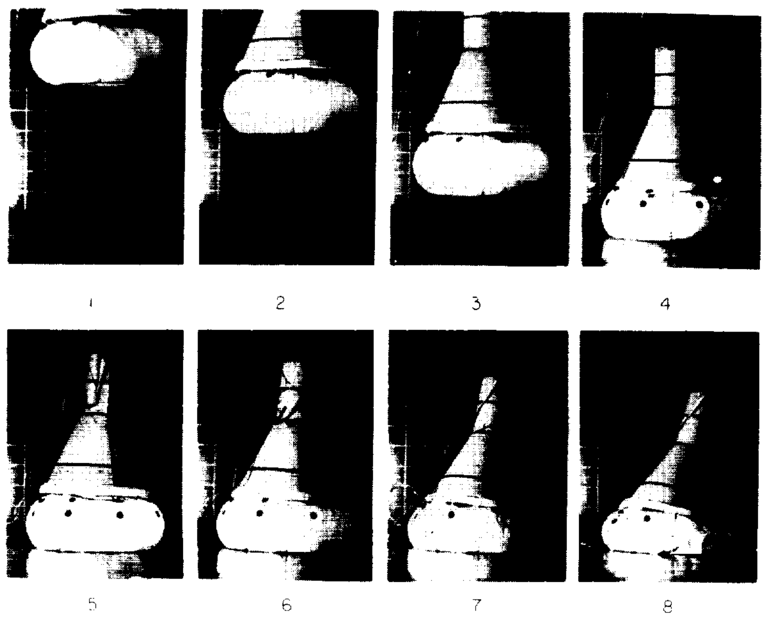

L-59-1501

Figure 5(a)

SEQUENCE OF TORUS BAG LANDINGS ON CONCRETE
FLIGHT-PATH ANGLE, 63°; CONTACT ATTITUDE, -26°

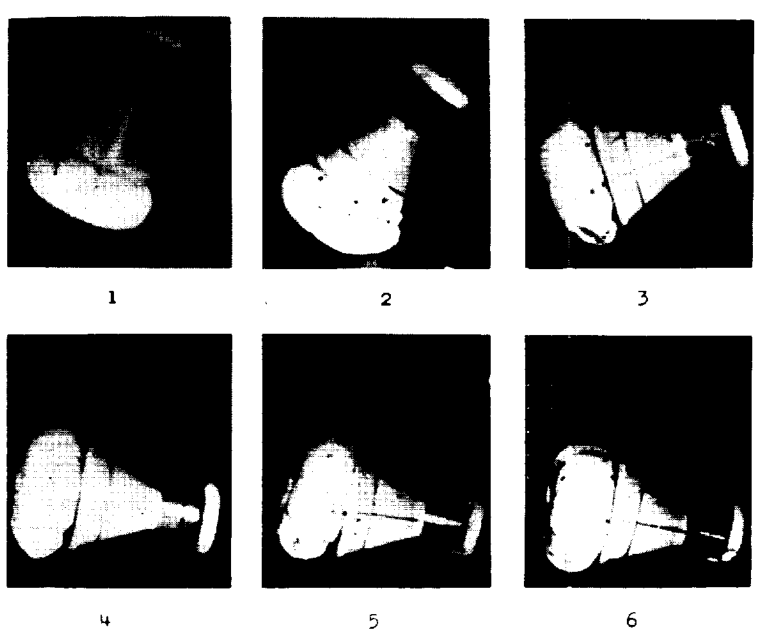

L-59-6105

Figure 5(b)

L-1082

L-1082

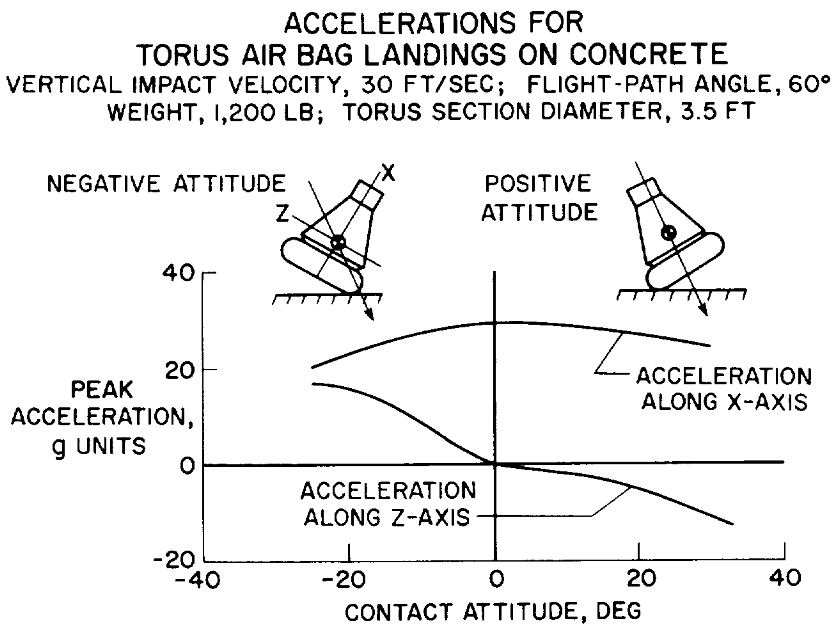

Figure 6

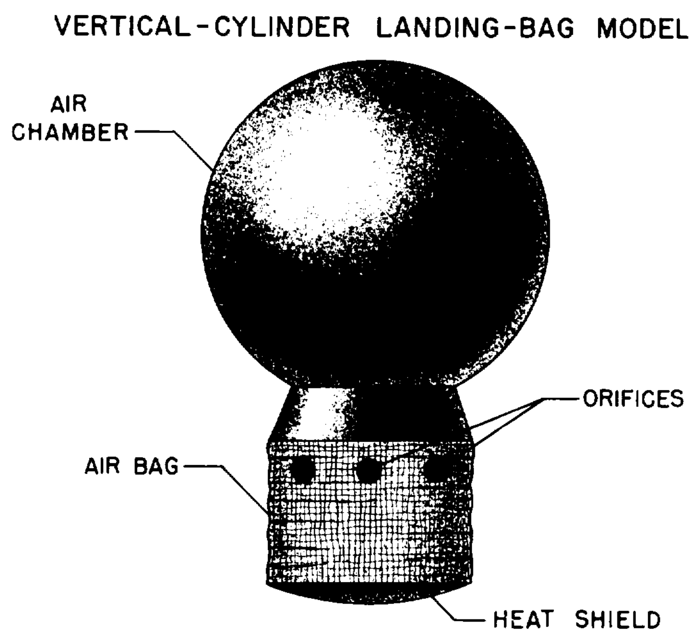

Figure 7

ACCELERATION TIME HISTORY FOR VERTICAL-CYLINDER BAG LANDING ON CONCRETE

IMPACT VELOCITY, 30 FT/SEC; FLIGHT-PATH ANGLE, 90°; CONTACT ATTITUDE, 0; WEIGHT, 2,000 LB

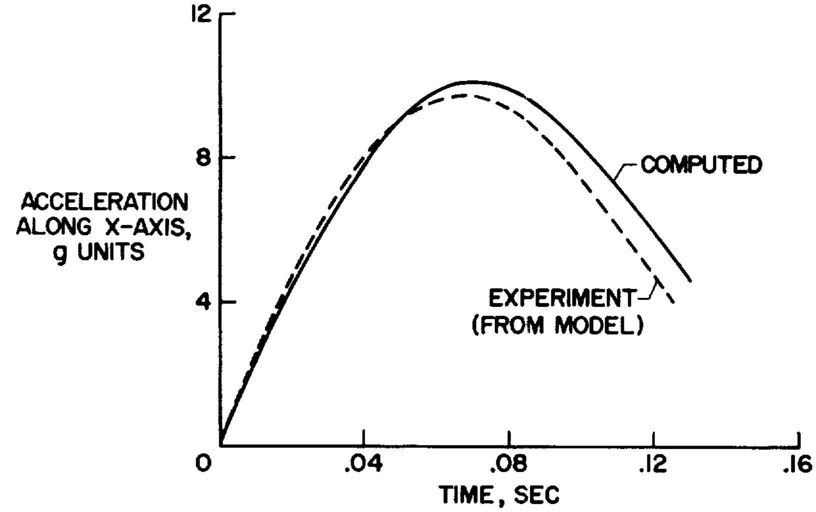

Figure 8

SMALL-SCALE COMPLIABLE-METAL-LEG MODEL

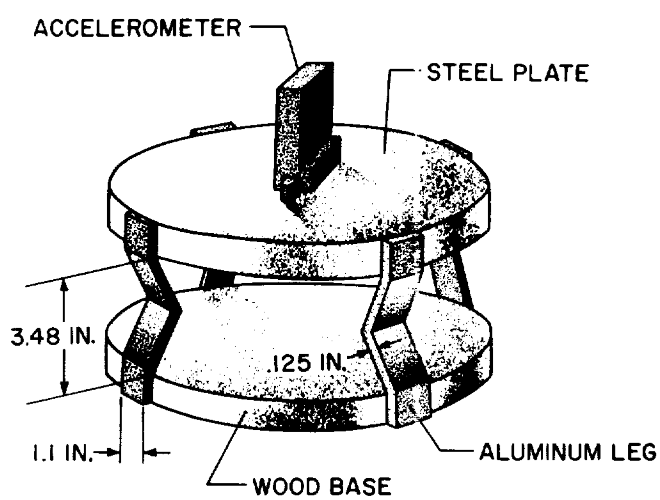

Figure 9

L-1082

L-1082

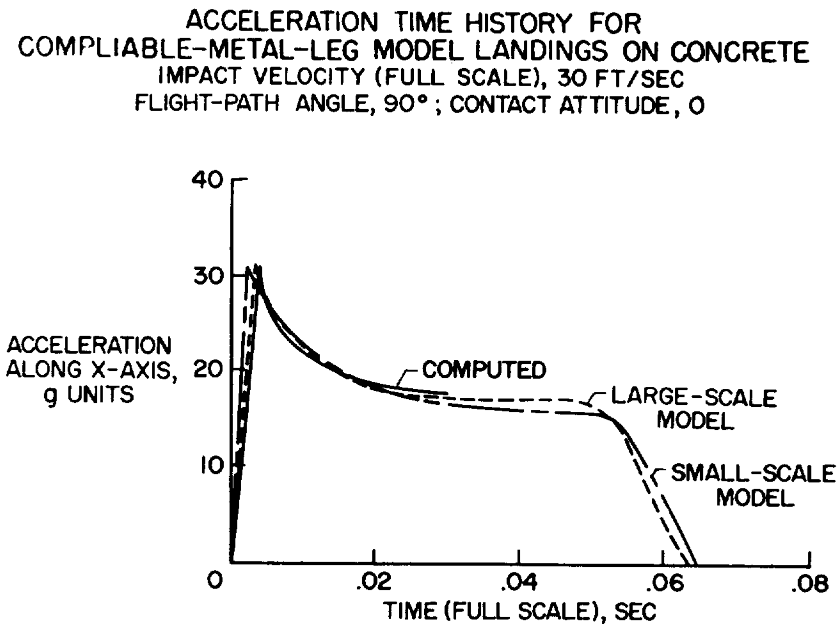

Figure 10

DYNAMIC MODEL WITH COMPLIABLE METAL LEGS BETWEEN CAPSULE AND HEAT SHIELD

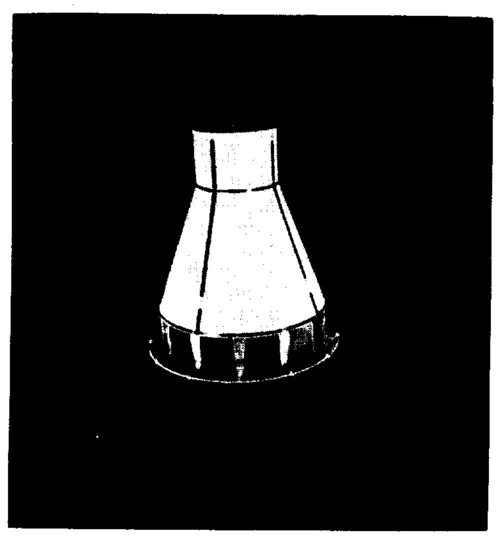

L-60-2464

Figure 11

SEQUENCE OF COMPLIABLE-METAL-LEG MODEL
LANDING ON CONCRETE
FLIGHT-PATH ANGLE, 90°; CONTACT ATTITUDE, 30°

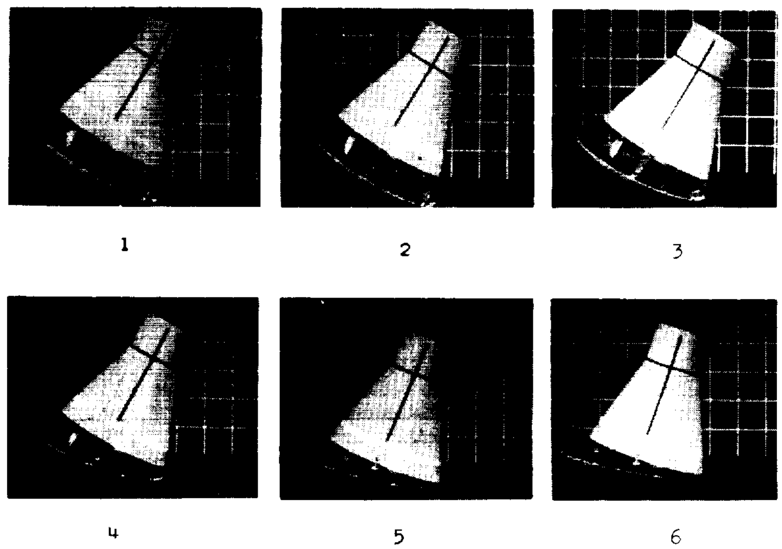

L-59-6203

Figure 12

ACCELERATIONS FOR CAPSULES LANDING ON WATER
IMPACT VELOCITY (FULL SCALE), 30 FT/SEC; FLIGHT-PATH ANGLE, 90°;
WEIGHT (FULL SCALE), 2,000 LB

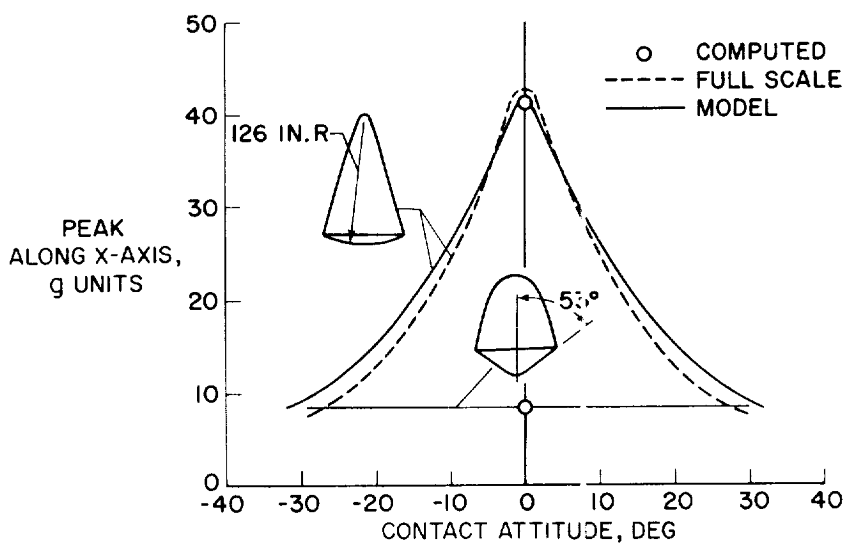

Figure 13

L-1082

SEQUENCE OF BRAKING-ROCKET MODEL LANDING ON CONCRETE

FLIGHT-PATH ANGLE, 60°

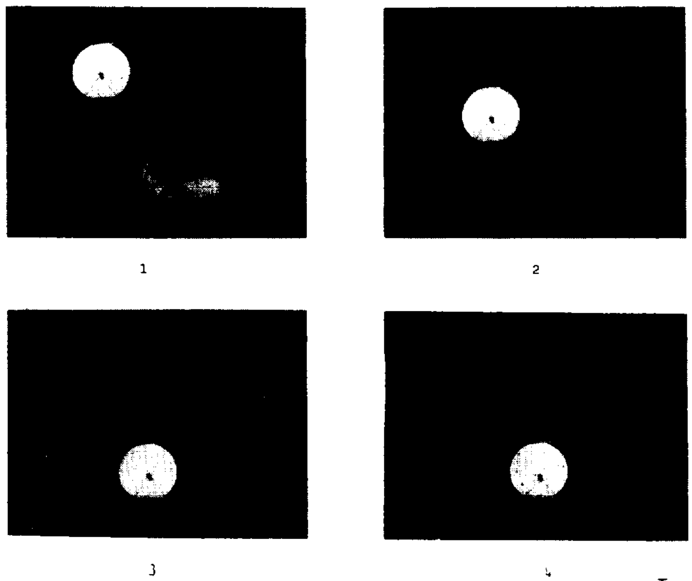

L-60-1899

Figure 14

DYNAMIC MODEL OF HORIZONTAL-LANDING REENTRY VEHICLE

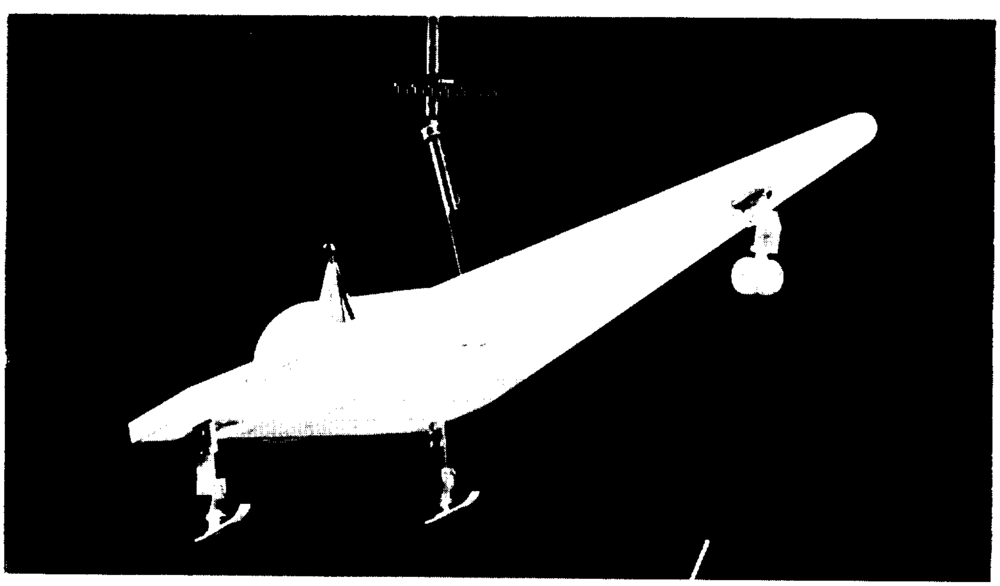

L-59-6533

Figure 15

SEQUENCE OF MODEL LANDING WITH MAIN-SKID NOSE-WHEEL LANDING GEAR

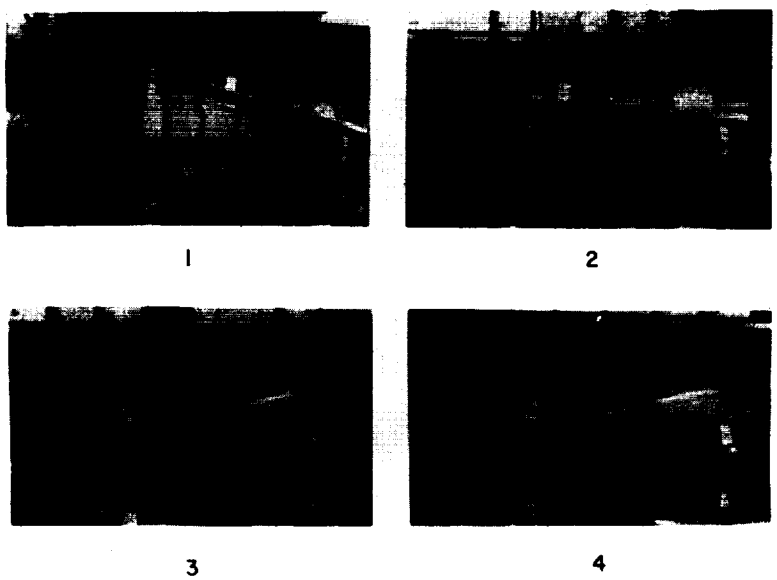

Figure 16 L-60-1720

LANDING TIME HISTORY

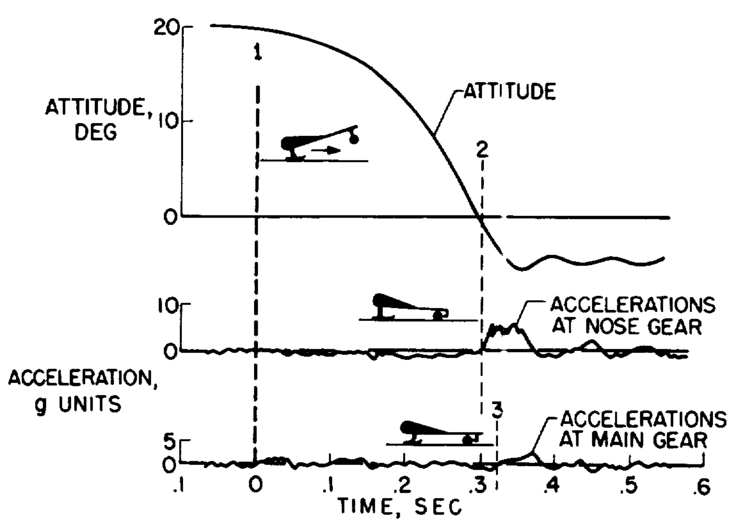

Figure 17